

Dispersive interactions between atoms and nonplanar surfacesRiccardo Messina,^{1,2} Diego A. R. Dalvit,³ Paulo A. Maia Neto,⁴ Astrid Lambrecht,¹ and Serge Reynaud¹¹*Laboratoire Kastler Brossel, case 74, CNRS, ENS, UPMC, Campus Jussieu, F-75252 Paris Cedex 05, France*²*Dipartimento di Scienze Fisiche e Astronomiche dell'Università degli Studi di Palermo and CNSIM, Via Archirafi 36, I-90123 Palermo, Italy*³*Theoretical Division, MS B213, Los Alamos National Laboratory, Los Alamos, New Mexico 87545, USA*⁴*Instituto de Física, UFRJ, CP 68528, Rio de Janeiro 21941-972, RJ, Brazil*

(Received 18 February 2009; published 27 August 2009)

We calculate the dispersive force between a ground-state atom and a nonplanar surface. We present explicit results for a corrugated surface, derived from the scattering approach at first order in the corrugation amplitude. A variety of analytical results in different limiting cases, including the van der Waals and Casimir-Polder regimes, is derived. We compute numerically the exact first-order dispersive potential for arbitrary separation distances and corrugation wavelengths for a rubidium atom on top of a silicon or gold corrugated surface. We discuss in detail the inadequacy of the proximity force approximation, and present a simple but adequate approximation for computing the potential.

DOI: [10.1103/PhysRevA.80.022119](https://doi.org/10.1103/PhysRevA.80.022119)

PACS number(s): 12.20.Ds, 03.75.Kk, 34.35.+a, 42.50.Ct

I. INTRODUCTION

Quantum and thermal fluctuations of the electromagnetic field in the presence of material boundaries generate fluctuating spatial gradients of the field intensity and fluctuating induced electric dipoles in ground-state atoms close to those surfaces, resulting in an atom-surface interaction via the optical dipole force. These dispersive forces have considerable importance in fundamental physics, including deflection of atomic beams close to surfaces [1], classical [2] and quantum reflections of cold atoms [3,4] and Bose-Einstein condensates (BECs) [5] from surfaces, dipole oscillations of BECs above dielectric surfaces [6,7], and in possible future applications of single-atom manipulation in atom chips [8,9]. At the limit of large separation distances {Casimir-Polder (CP) limit [10]}, the interaction show universal features since it depends only on the zero-frequency atom and surface optical responses.

Dispersive forces can be tailored in different ways, either by engineering the optical properties of the surfaces [11–13], by biasing the temperatures of the surfaces and their thermal environment [7,14,15], or by suitably changing their geometry. Given the complexity of these quantum forces, which arise from fluctuations at all frequency and length scales, calculations beyond planar geometries are exceedingly involved. Until recently, approximate methods have been used to deal with nonplanar setups, including the proximity force approximation (PFA) [16] and the pairwise summation approach (PWS) [17]. However, these approximate methods drastically fail when the surface is not sufficiently smooth on the length scale of the atom-surface separation since they do not properly take into account the nonadditivity of dispersion forces [18]. These large deviations from PFA or PWS could be probed by using present-day technology, for example, with a Bose-Einstein condensate above a microfabricated corrugated surface [19]. Similar deviations have been recently measured for the Casimir force between a metallic sphere and a nanostructured silicon rectangular grating [20,21].

A number of methods are available for computing the dispersive atom-surface forces (see, for example, [10,22–25]). These methods allow the exact computation of the force for very simple geometries, such as an atom above a single (possibly multilayered) plane, sphere, or cylinder, or an atom inside a plane Fabry-Perot cavity. Toy models with scalar fields with ideal (Dirichlet) boundary conditions have also been considered in computing the “scalar Casimir-Polder” force for a small sphere above a uniaxial corrugated surface [26].

Similar problems have been discussed for the Casimir interaction between two macroscopic bodies (see, for example, [27–29]), and the scattering approach has been shown to be a very efficient tool for analyzing the case of nontrivial geometries [30]. For parallel plates, the Casimir force may be written in terms of the reflection coefficients seen from the region in between the plates [31,32]. A similar expression also holds for nonplanar surfaces, with the specular reflection coefficients replaced by more general reflection operators that describe nonspecular diffraction by the surfaces. This allows for the computation of the Casimir force between rough [33] or corrugated [34] surfaces. Similar methods have been employed to compute the force between a plane and a sphere [35–38], and between two spheres [39,40].

In this paper we develop the scattering approach for studying the dispersive interaction between ground-state atoms and arbitrarily shaped surfaces characterized by frequency-dependent reflection operators. This approach provides an exact analytical expression for the two-body interaction energy, which can be written in terms of the scattering matrices defined for each individual one-body scatterer. Although this is a simpler problem than solving for the many-body Green function, it is still very difficult to find the exact scattering matrices for the problem of a electromagnetic field impinging on a given nonplanar geometry. In order to illustrate the method, we write the two-body interaction energy in a perturbative expansion in terms of the deviation of the surface profile from the planar case [19]. Apart from this perturbative approximation, the approach is valid for any value of the corrugation wavelength, and includes the full

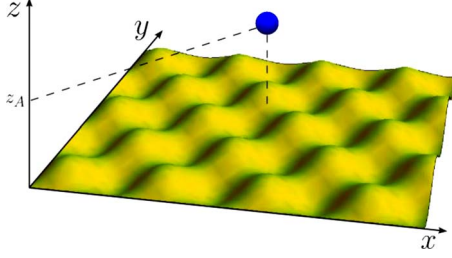


FIG. 1. (Color online) Ground-state atom on top of a nonplanar surface [profile function $h(x, y)$].

electromagnetic fluctuations and the real material properties of the boundaries. We compute the perturbative dispersive interaction potential to first order in the surface profile both for ideal and real materials, and discuss the prospects of measuring nontrivial (beyond-PFA) geometrical effects with a uniaxial corrugated surface interacting with a Bose-Einstein condensate used as a vacuum field sensor.

The paper is organized in the following way. In Sec. II, we develop the scattering formalism for the atom-surface interaction. The resulting general formula is then applied to calculate the potential to first order in the surface corrugation amplitude in Sec. III. We compare our results with PFA in Sec. IV and discuss experimental prospects in Sec. V. Concluding remarks are presented in Sec. VI.

II. ATOM-SURFACE INTERACTION FOR NONPLANAR GEOMETRIES

We consider a ground-state atom at position $\mathbf{R}_A = (\mathbf{r}_A, z_A)$ on top of a nonplanar surface, as shown by Fig. 1. The surface profile is defined by the function $h(x, y)$ representing the local height with respect to the plane $z=0$. The atom is in free space so that $z_A > h(\mathbf{r}_A)$. The fluctuating electromagnetic field propagating from the surface toward the atom is written in the mixed Fourier representation (frequency ω , two-dimensional wave vector \mathbf{k})

$$\mathbf{E}^\dagger(\mathbf{k}, z, \omega) = \sum_{p=\text{TE, TM}} E_p^\dagger(\mathbf{k}, \omega) \hat{\mathbf{e}}_p^+(\mathbf{k}, \omega) e^{ik_z z}, \quad (1)$$

where p is the polarization index and k_z is the longitudinal wave vector (sgn denotes the sign function; $k = |\mathbf{k}|$)

$$k_z = \text{sgn}(\omega) \sqrt{\omega^2/c^2 - k^2}.$$

Similar expressions in terms of unit vectors $\hat{\mathbf{e}}_{\text{TE}}^-$ and $\hat{\mathbf{e}}_{\text{TM}}^-$ hold for the field $\mathbf{E}^\dagger(\mathbf{k}, z, \omega)$ propagating toward the surface, with the replacement $k_z \rightarrow -k_z$. The complete wave vector is denoted as $\mathbf{K}^\pm = \mathbf{k} \pm k_z \hat{\mathbf{z}}$, and the unit vectors are given by (the frequency dependence will be generally omitted)

$$\begin{aligned} \hat{\mathbf{e}}_{\text{TE}}^+(\mathbf{k}) &= \hat{\mathbf{e}}_{\text{TE}}^-(\mathbf{k}) = \hat{\mathbf{z}} \times \hat{\mathbf{k}}, \\ \hat{\mathbf{e}}_{\text{TM}}^+(\mathbf{k}) &= \hat{\mathbf{e}}_{\text{TM}}^-(\mathbf{k}) \times \hat{\mathbf{K}}^\pm, \end{aligned} \quad (2)$$

corresponding to transverse electric (TE) and transverse magnetic (TM) polarizations, respectively.

The reflection by the nonplanar surface modifies the wave vector \mathbf{k} and the polarization $p = \text{TE, TM}$, while conserving

the frequency ω since the surface is assumed to be stationary

$$E_p^\dagger(\mathbf{k}, \omega) = \int \frac{d^2 \mathbf{k}'}{(2\pi)^2} \sum_{p'} \langle \mathbf{k}, p | \mathcal{R}_S(\omega) | \mathbf{k}', p' \rangle E_{p'}^\dagger(\mathbf{k}', \omega). \quad (3)$$

The reflection operator $\mathcal{R}_S(\omega)$ depends on the surface-profile function $h(x, y)$. Explicit results for its matrix elements are presented in Sec. III to first order in $h(x, y)$.

Let us assume for a moment that the z axis is taken along the atom position ($\mathbf{r}_A = \mathbf{0}$). At zero temperature, the Casimir atom-surface interaction energy is then given by the zero-temperature scattering formula as an integral over the positive imaginary frequency axis ($\omega \rightarrow i\xi$) (see [30])

$$\begin{aligned} U(\mathbf{R}_A) &= \hbar \int_0^\infty \frac{d\xi}{2\pi} \text{Tr} \log(1 - \mathcal{R}_S e^{-\mathcal{K}z_A} \mathcal{R}_A e^{-\mathcal{K}z_A}), \\ \mathcal{K} &= \text{diag}(\kappa), \quad \kappa = \sqrt{\xi^2/c^2 + k^2}, \end{aligned} \quad (4)$$

with \mathcal{R}_A and \mathcal{R}_S representing the reflection operators for the atom and the surface, respectively. \mathcal{K} is a diagonal operator in the basis of plane waves $|\mathbf{k}, p\rangle$ with eigenvalues κ so that $e^{-\mathcal{K}z_A}$ represents the propagation between the two scatterers. Alternatively, it may also be interpreted as the displacement operator [39]: here \mathcal{R}_A is computed for a coordinate axis centered at the atom center of mass, whereas $e^{-\mathcal{K}z_A} \mathcal{R}_A e^{-\mathcal{K}z_A}$ corresponds to the ‘‘laboratory’’ axis. A similar expression holds at finite temperature, replacing the integral over imaginary frequencies ξ by a sum over Matsubara frequencies.

It is actually simple to calculate the atomic reflection operator for an arbitrary position (\mathbf{r}_A, z_A) when taking the plane-wave basis. The spherically symmetric ground-state atom is described as an induced electric dipole, with a dipole moment

$$\mathbf{d}(\omega) = \alpha(\omega) \mathbf{E}(\mathbf{R}_A, \omega). \quad (5)$$

Let us emphasize at this point that $\alpha(\omega)$ is the dynamic polarizability defined according to SI unit system [41]. Induced dipole (5) produces an electric field given by

$$\mathbf{E}_{(\text{dip})}(\mathbf{R}, \omega) = \frac{1}{4\pi\epsilon_0} \nabla \times \nabla \times \left[\mathbf{d}(\omega) \frac{\exp\left(i\frac{\omega}{c} R'\right)}{R'} \right], \quad (6)$$

where $\mathbf{R}' = \mathbf{R} - \mathbf{R}_A$ and ∇ represents the spatial gradient. In order to derive a representation of the outgoing field analogous to Eq. (1), we make use of Weyl’s plane-wave expansion of a spherical wave [42], considering only the field propagating in the region $z < z_A$, and projecting on the polarization unit vectors defined by Eq. (2), obtaining [43]

$$E_{(\text{dip})p}^\dagger(\mathbf{k}, \omega) = \frac{i\omega^2}{2\epsilon_0 c^2 k_z} \hat{\mathbf{e}}_p^-(\mathbf{k}) \cdot \mathbf{d}(\omega) e^{-i\mathbf{k} \cdot \mathbf{r}_A} e^{ik_z z_A}. \quad (7)$$

When replacing Eq. (5) into Eq. (7), we find two separate contributions associated to the field Fourier components propagating upward or downward. To calculate the atom reflection operator, we take the upward components

$$E_{(\text{dip})p}^\downarrow(\mathbf{k}, \omega) = \frac{i\omega^2\alpha(\omega)}{2\epsilon_0 c^2 k_z} \int \frac{d^2\mathbf{k}'}{(2\pi)^2} \sum_{p'} \hat{\boldsymbol{\epsilon}}_p^-(\mathbf{k}) \cdot \hat{\boldsymbol{\epsilon}}_{p'}^+(\mathbf{k}') \times e^{-i(\mathbf{k}-\mathbf{k}')\cdot\mathbf{r}_A} e^{i(k_z+k'_z)z_A} E_{p'}^\uparrow(\mathbf{k}', \omega). \quad (8)$$

This result can be cast into a form similar to Eq. (3), with the atomic reflection operator given by ($\omega \rightarrow i\xi$ and $k_z \rightarrow i\kappa$)

$$\langle \mathbf{k}, p | \mathcal{R}_A | \mathbf{k}', p' \rangle = -\frac{\xi^2}{2\kappa} \frac{\alpha(i\xi)}{\epsilon_0 c^2} \hat{\boldsymbol{\epsilon}}_p^-(\mathbf{k}) \cdot \hat{\boldsymbol{\epsilon}}_{p'}^+(\mathbf{k}') \times e^{-i(\mathbf{k}-\mathbf{k}')\cdot\mathbf{r}_A} e^{-(\kappa+\kappa')z_A}. \quad (9)$$

The dependence on \mathbf{r}_A and z_A in this equation is exactly the one expected from the matrix elements of the displacement operator in the plane-wave basis. The displacement along the z axis was already explicitly taken into account in scattering formula (4) so we must take $z_A=0$ when replacing Eq. (9) into Eq. (4).

As we assume that the atom-surface separation distance is much larger than the atomic dimensions, we may expand the general scattering formula (4) to first order in $\alpha(\omega)$ or, equivalently, to first order in \mathcal{R}_A [44]

$$U(\mathbf{R}_A) = -\hbar \int_0^\infty \frac{d\xi}{2\pi} \int \frac{d^2\mathbf{k}}{(2\pi)^2} \int \frac{d^2\mathbf{k}'}{(2\pi)^2} e^{-(\kappa+\kappa')z_A} \times \sum_{p,p'} \langle \mathbf{k}, p | \mathcal{R}_S | \mathbf{k}', p' \rangle \langle \mathbf{k}', p' | \mathcal{R}_A | \mathbf{k}, p \rangle. \quad (10)$$

The z_A dependence is already explicit in Eq. (10) because \mathcal{R}_A in Eq. (4) was defined with respect to the reference axis such that $z_A=0$. Note that the resulting z_A dependence coincides with Eq. (9), which was derived for an arbitrary position with respect to the origin. From Eqs. (9) and (10), we find

$$U(\mathbf{R}_A) = \frac{\hbar}{\epsilon_0 c^2} \int_0^\infty \frac{d\xi}{2\pi} \xi^2 \alpha(i\xi) \int \frac{d^2\mathbf{k}}{(2\pi)^2} \int \frac{d^2\mathbf{k}'}{(2\pi)^2} \times \frac{e^{i(\mathbf{k}-\mathbf{k}')\cdot\mathbf{r}_A} e^{-(\kappa+\kappa')z_A}}{2\kappa'} \times \sum_{p,p'} \langle \mathbf{k}, p | \mathcal{R}_S | \mathbf{k}', p' \rangle \hat{\boldsymbol{\epsilon}}_p^+(\mathbf{k}) \cdot \hat{\boldsymbol{\epsilon}}_{p'}^-(\mathbf{k}'). \quad (11)$$

Note that this general formula holds for magnetodielectric media, including the anisotropic case [11]. The dispersive potential for an atom with magnetic polarizability [45] can also be derived from Eq. (4) along the lines presented above. The corresponding atomic reflection operator is calculated in Appendix A.

As a first application of Eq. (11), we briefly consider the case of a planar surface at $z=0$ [corresponding to a profile function $h(x,y)=0$] made of some isotropic material. In this case, \mathcal{R}_S is diagonal, its matrix elements being

$$\langle \mathbf{k}, p | \mathcal{R}_S | \mathbf{k}', p' \rangle = (2\pi)^2 \delta^{(2)}(\mathbf{k}-\mathbf{k}') \delta_{p,p'} r^p(k, i\xi), \quad (12)$$

where $r^p(k, i\xi)$ are the specular reflection coefficients for the plane surface. For instance, for a homogeneous nonmagnetic bulk medium, they are given by the Fresnel formulas [$\epsilon(i\xi)$ = electric permittivity]

$$r^{\text{TE}}(\mathbf{k}, i\xi) = \frac{\kappa - \kappa_t}{\kappa + \kappa_t}, \quad r^{\text{TM}}(\mathbf{k}, i\xi) = \frac{\epsilon(i\xi)\kappa - \kappa_t}{\epsilon(i\xi)\kappa + \kappa_t}, \quad \kappa_t = \sqrt{k^2 + \epsilon(i\xi)\xi^2/c^2}. \quad (13)$$

Equation (11) then yields the known interaction energy between a ground-state atom and a plane surface valid for arbitrary separation distances [22–25,29]

$$U^{(0)}(z_A) = \frac{\hbar}{\epsilon_0 c^2} \int_0^\infty \frac{d\xi}{2\pi} \xi^2 \alpha(i\xi) \int \frac{d^2\mathbf{k}}{(2\pi)^2} \frac{e^{-2\kappa z_A}}{2\kappa} \times \left[r^{\text{TE}}(\mathbf{k}, i\xi) - \left(1 + \frac{2c^2 k^2}{\xi^2} \right) r^{\text{TM}}(\mathbf{k}, i\xi) \right]. \quad (14)$$

This expression can be simplified under the assumption of small or large distances z_A (with respect to some typical atomic transition wavelength λ_A). For $z_A \ll \lambda_A$ and $z_A \gg \lambda_A$, we get the van der Waals (vdW) and Casimir-Polder limits that correspond, respectively, to Eqs. (24) and (22) in Ref. [46].

Equation (11) represents a general result for the dispersive interaction between an atom and a body scatterer. The difficulty, of course, lies in the explicit derivation of the matrix elements of the corresponding operator \mathcal{R}_S . In the next section, we apply this result to derive the lateral dispersive force for an atom on top of a corrugated surface up to first order in the corrugation profile $h(\mathbf{r})$. A second interesting application, left for a future publication, would be to compute the roughness correction to the normal dispersive force—in this case it is necessary to compute \mathcal{R}_S up to second order in $h(\mathbf{r})$ (see [33]).

III. PERTURBATIVE INTERACTION POTENTIAL WITHIN THE SCATTERING APPROACH

In order to compute the exact atom-surface interaction potential it is necessary to find the reflection operators of the surface, which is a highly nontrivial problem. For the sake of illustration of the scattering formalism applied to the atom-surface problem, we now compute those reflection operators in a perturbative expansion in terms of the deviations $h(\mathbf{r})$ of the surface profile with respect to the planar configuration. We will calculate the atom-surface interaction energy to first order in h . This term gives rise both to a correction to the normal force and to a lateral force on the atom, which does not exist in the case of a planar surface. We start by expanding the reflection operators in powers of h as $\mathcal{R} = \mathcal{R}^{(0)} + \mathcal{R}^{(1)} + O(h^2)$. We model the optical response of the homogeneous isotropic material in terms of its frequency-dependent electric permittivity $\epsilon(\omega)$. The zeroth-order term $\mathcal{R}^{(0)}$ is given by Eq. (12), whereas the first-order reflection matrix elements can be written as

$$\langle \mathbf{k}, p | \mathcal{R}^{(1)} | \mathbf{k}', p' \rangle = R_{pp'}^{(1)}(\mathbf{k}, \mathbf{k}') H(\mathbf{k} - \mathbf{k}'), \quad (15)$$

where $H(\mathbf{k})$ is the Fourier transform of the surface profile $h(\mathbf{r})$. Therefore, the first-order atom-surface interaction potential is

$$U^{(1)}(\mathbf{R}_A) = \int \frac{d^2\mathbf{k}}{(2\pi)^2} e^{i\mathbf{k}\cdot\mathbf{r}_A} g(\mathbf{k}, z_A) H(\mathbf{k}), \quad (16)$$

where $g(\mathbf{k}, z_A)$ is the response function

$$g(\mathbf{k}, z_A) = \frac{\hbar}{\epsilon_0 c^2} \int_0^\infty \frac{d\xi}{2\pi} \xi^2 \alpha(i\xi) \int \frac{d^2\mathbf{k}'}{(2\pi)^2} a_{\mathbf{k}', \mathbf{k}''},$$

$$a_{\mathbf{k}', \mathbf{k}''} = \frac{e^{-(\kappa' + \kappa'')z_A}}{2\kappa''} \times \sum_{p', p''} \hat{\boldsymbol{\epsilon}}_{p'}^+(\mathbf{k}') \cdot \hat{\boldsymbol{\epsilon}}_{p''}^-(\mathbf{k}'') R_{p'p''}^{(1)}(\mathbf{k}', \mathbf{k}''). \quad (17)$$

The first-order reflection matrix was calculated in [33] by following the approach presented in [47] (see also [48]). It is a nondiagonal matrix with nonspecular reflection coefficients given by

$$R_{pp'}^{(1)}(\mathbf{k}, \mathbf{k}') = u_{pp'}(k, k'; i\xi) \Lambda_{pp'}^{(1)}(\mathbf{k}, \mathbf{k}'; i\xi), \quad (18)$$

where we have defined

$$u_{pp'}(k, k'; i\xi) = \frac{t^p(k, i\xi) t^{p'}(k', i\xi)}{t^p(k, i\xi)}. \quad (19)$$

$t^p(\mathbf{k}, i\xi)$ are the transmission Fresnel coefficients for the planar interface defined by

$$t^{\text{TE}}(\mathbf{k}, i\xi) = \frac{2\kappa}{\kappa + \kappa_t}, \quad t^{\text{TM}}(\mathbf{k}, i\xi) = \frac{2\sqrt{\epsilon(i\xi)}\kappa}{\epsilon(i\xi)\kappa + \kappa_t}. \quad (20)$$

The matrix $\Lambda^{(1)}$ is expressed as $\Lambda^{(1)} = \Lambda_+^{(1)} - \Lambda_-^{(1)}$ with

$$\Lambda_{\pm}^{(1)}(\mathbf{k}, \mathbf{k}'; i\xi) = (\kappa_t \pm \kappa) \mathbf{B}_t^{-1} \begin{pmatrix} C & S \\ -S & C \pm \beta\beta_t' \end{pmatrix} \mathbf{B}_t',$$

with

$$\mathbf{B}_t = \text{diag}[1, c\kappa_t/\sqrt{\epsilon(i\xi)}\xi], \quad \beta = k/\kappa, \quad \beta_t = k/\kappa_t, \\ C = \cos(\phi - \phi'), \quad S = \sin(\phi - \phi'). \quad (21)$$

We have denoted with ϕ (ϕ') the angle between \mathbf{k} (\mathbf{k}') and an arbitrarily chosen axis on the surface plane. Starting from these definitions and using the scalar product of polarization vectors

$$\hat{\boldsymbol{\epsilon}}_{\text{TE}}^+(\mathbf{k}) \cdot \hat{\boldsymbol{\epsilon}}_{\text{TE}}^-(\mathbf{k}') = C, \\ \hat{\boldsymbol{\epsilon}}_{\text{TE}}^+(\mathbf{k}) \cdot \hat{\boldsymbol{\epsilon}}_{\text{TM}}^-(\mathbf{k}') = \frac{c\kappa'S}{\xi}, \\ \hat{\boldsymbol{\epsilon}}_{\text{TM}}^+(\mathbf{k}) \cdot \hat{\boldsymbol{\epsilon}}_{\text{TE}}^-(\mathbf{k}') = \frac{c\kappa S}{\xi}, \\ \hat{\boldsymbol{\epsilon}}_{\text{TM}}^+(\mathbf{k}) \cdot \hat{\boldsymbol{\epsilon}}_{\text{TM}}^-(\mathbf{k}') = -\frac{c^2}{\xi^2}(kk' + \kappa\kappa'C), \quad (22)$$

we obtain for $a_{\mathbf{k}', \mathbf{k}''}$ the following general expression

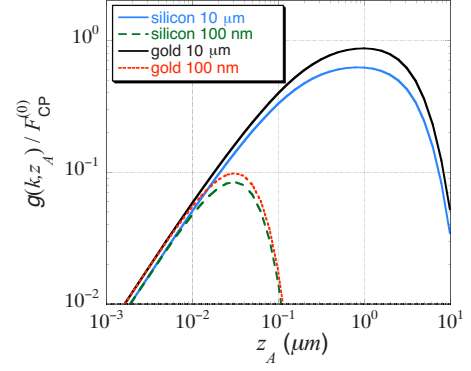


FIG. 2. (Color online) Dimensionless ratio $g(k, z_A)/F_{\text{CP}}^{(0)}(z_A)$ as a function of separation distance z_A (for a ground-state Rb atom). For the corrugation wavelength $\lambda = 2\pi/k = 10 \mu\text{m}$, we show the values for gold (black) and silicon (blue/gray) surfaces. We also show the results for $\lambda = 100 \text{ nm}$ with gold (dotted) and silicon (dashed) surfaces.

$$a_{\mathbf{k}', \mathbf{k}''} = e^{-(\kappa' + \kappa'')z_A} \frac{\kappa'}{\kappa''} \left[C^2 u_{\text{TE,TE}} + \frac{\kappa'' \kappa_t' S^2}{\sqrt{\epsilon(i\xi)} \xi^2 / c^2} u_{\text{TE,TM}} \right. \\ \left. + \frac{\sqrt{\epsilon(i\xi)} \kappa' \kappa_t' S^2}{\xi^2 / c^2 - (\kappa')^2 [\epsilon(i\xi) + 1]} u_{\text{TM,TE}} \right. \\ \left. + \frac{[k'k'' + \kappa' \kappa'' C] [\epsilon(i\xi) k'k'' + \kappa_t' \kappa_t'' C]}{(\xi^2 / c^2) \{ \xi^2 / c^2 - (\kappa')^2 [\epsilon(i\xi) + 1] \}} u_{\text{TM,TM}} \right]. \quad (23)$$

By inspection of Eq. (23), one shows that the response function $g(\mathbf{k}, z_A)$ depends only on the modulus $k = |\mathbf{k}|$ of the corrugation wave vector, as expected: the information about the direction associated to the surface profile is contained only in $H(\mathbf{k})$, whereas the response function derived within the perturbative approach is based on the planar geometry and its underlying symmetry.

The results presented above allow for the numerical calculation of the first-order potential for arbitrary ground-state atoms and material media by plugging the numerical data for the corresponding polarizability and permittivity functions into Eqs. (17) and (23). As an illustration, we consider a ground-state rubidium atom above a gold or a silicon surface. The numerical data for the dynamical atomic polarizability at imaginary frequencies, $\alpha(i\xi)$, were kindly provided by Derevianko *et al.* [49] (these same data are plotted in Fig. 9 of [46]). The numerical values for the optical data at real frequencies for gold and silicon were obtained from the handbook of optical data [50]. For silicon the available data cover the whole necessary frequency range while for gold the data need to be completed at low frequencies, using a standard Drude model with a dielectric permittivity $\epsilon(\omega) = 1 - \omega_p^2 / [\omega(\omega + i\gamma)]$ with a plasma frequency $\omega_p = 9 \text{ eV}$ and a relaxation rate $\gamma = 35 \text{ meV}$ [51]. The values along the imaginary frequency axis were then calculated with the help of dispersion relations [52].

In Fig. 2, we plot the response function after normalizing it by

$$F_{\text{CP}}^{(0)}(z_A) = -\frac{3\hbar c \alpha(0)}{8\pi^2 \epsilon_0 z_A^5}, \quad (24)$$

which is also the result derived by Casimir and Polder [10] for the attractive force on an atom on top of a perfectly reflecting plate at large separation distances. The horizontal axis represents the atom-surface separation z_A . We take two different values of k , corresponding to corrugation wavelengths $\lambda = 2\pi/k = 10 \mu\text{m}$ and 100 nm .

The global shape of the curves can be discussed in a qualitative manner, which will be made more quantitative later on. At low values of kz_A , PFA is expected to hold so that the response is approximately independent of k . The ratio thus grows linearly with z , showing the well-known power-law change when sweeping from the unretarded van der Waals to the retarded Casimir-Polder regime. As z_A approaches $1/k$, PFA becomes gradually worse, and then a non-trivial geometry effect reduces $g(k, z_A)$ exponentially for $z_A \gg 1/k$. In the next section, we show that geometry and real material effects can be disentangled in most cases of interest, thus providing a simple manner to explain how they jointly produce the results shown in Fig. 2.

IV. DISENTANGLING GEOMETRY AND REAL MATERIAL EFFECTS

As discussed in Sec. I, the most commonly used approximation methods to compute atom-surface interactions are the PFA and PWS. In [18] we compared these approximate methods with our exact scattering approach to first-order in the surface profile for the case of perfect reflectors, and showed that PFA overestimates and PWS underestimates the lateral atom-surface force. In this section we want to expand upon these considerations and consider in further detail the corrections to the PFA approximation beyond the case of perfect reflection. This will allow us to disentangle the effects of geometry and real materials, thus leading to a very simple rule for the evaluation of $g(k, z_A)$.

In the atom-surface context, the proximity force approximation amounts to computing the atom-surface potential U for a given geometry from the potential for the planar geometry $U^{(0)}$ taken at the local atom-surface distance

$$U \simeq U^{(0)}[z_A - h(\mathbf{r}_A)] \simeq U^{(0)} - h(\mathbf{r}_A) \partial_z U^{(0)}.$$

The PFA holds when the surface is very smooth in the scale of the separation distance, which corresponds to the limit $kz_A \rightarrow 0$. From our expression for the first-order potential (16) one can indeed prove that for any material the response function satisfies the ‘‘proximity force theorem’’

$$g(k=0, z_A) = -\partial_z U^{(0)}(z_A). \quad (25)$$

This follows from the fact that the response function at zero transverse momentum is given by the specular limit of the nonspecular coefficients $a_{\mathbf{k}', \mathbf{k}''}$, which corresponds to $\mathbf{k}' = \mathbf{k}''$. In this case we have $R_{p', p''}^{(1)}(\mathbf{k}', \mathbf{k}') = 2\kappa' r^{p'}(\mathbf{k}'; i\xi) \delta_{p', p''}$, and $a_{\mathbf{k}', \mathbf{k}'} = e^{-2\kappa z_A} \sum_{p'} \hat{\epsilon}_p^+(\mathbf{k}') \cdot \hat{\epsilon}_p^-(\mathbf{k}') r^{p'}(\mathbf{k}'; i\xi)$. From Eq. (17), the zero-momentum response function is then

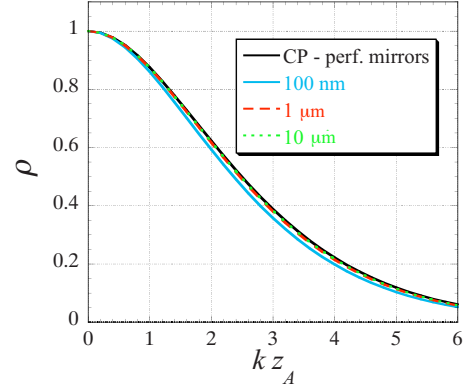


FIG. 3. (Color online) Geometry correction factor ρ as a function of kz_A for a silicon surface, and $z_A = 100 \text{ nm}$ (light blue/gray), $1 \mu\text{m}$ (dashed), and $10 \mu\text{m}$ (dotted). The black line corresponds to the CP result given by Eq. (29).

$$g(k=0, z_A) = \frac{\hbar}{\epsilon_0 c^2} \int_0^\infty \frac{d\xi}{2\pi} \xi^2 \alpha(i\xi) \int \frac{d^2\mathbf{k}}{(2\pi)^2} e^{-2\kappa z_A} \times \sum_p \hat{\epsilon}_p^+(\mathbf{k}) \cdot \hat{\epsilon}_p^-(\mathbf{k}) r^p(\mathbf{k}; i\xi). \quad (26)$$

Comparing with expression (14) for $U^{(0)}$, we immediately prove the proximity force theorem (25).

As a consequence of this discussion, we recover Eq. (25) from our more general result [Eq. (16)] when replacing $g(k, z_A)$ by $g(0, z_A)$. Now the value of $g(k, z_A)$ differs from $g(0, z_A)$ for any finite value of k and it is worth quantifying deviations from PFA by introducing the function

$$\rho(k, z_A) = \frac{g(k, z_A)}{g(0, z_A)}. \quad (27)$$

Deviations from PFA can first be discussed in the vicinity of $k=0$ where PFA is recovered ($\rho \rightarrow 1$ for $k \rightarrow 0$). It is possible to deduce from Eqs. (17)–(23) that the first-order derivative of ρ with respect to k is identically zero, for any atomic polarizability and surface permittivity. It follows that deviations from PFA appear only at order k^2 in a Taylor expansion around $k=0$

$$\rho(k, z_A) = 1 + \frac{k^2}{2} \partial_k^2 \rho(0, z_A) + O(k^3). \quad (28)$$

For perfect reflectors, we can also prove that the second-order derivative in Eq. (28) is negative so that $\rho(k, z_A)$ is concave near $k=0$.

When going far beyond PFA (arbitrary values of kz_A), we have to compute $\rho(k, z_A)$ numerically. The result of this calculation is plotted on Fig. 3, with ρ shown as a function of kz_A for three different values of z_A in the case of an Rb atom on top of a Si surface. We notice that these curves are quite close to one another. In order to obtain an estimate of their values, we also show the curve corresponding to the Casimir-Polder limit for perfect reflectors, which is derived from Eq. (27) and the calculations of Appendix B

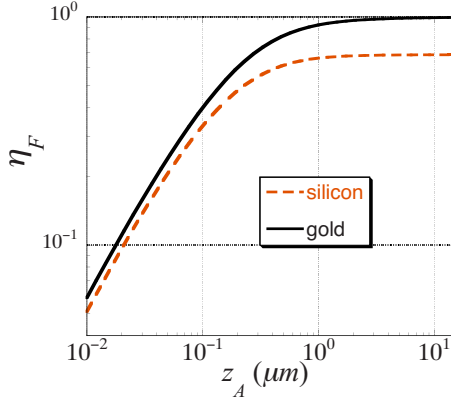


FIG. 4. (Color online) Correction $\eta_F = F^{(0)}/F_{\text{CP}}^{(0)}$ of the normal dispersive force between a Rb ground-state atom and a plane gold (solid) or silicon (dashed) surface as a function of the separation distance z_A .

$$\rho_{\text{CP}}^{\text{perf}}(k, z_A) = e^{-kz_A} \left(1 + kz_A + \frac{16(kz_A)^2}{45} + \frac{(kz_A)^3}{45} \right). \quad (29)$$

For this limiting case, ρ depends only on the dimensionless variable $\mathcal{Z} = kz_A$. We may thus conclude that this variable captures most of the geometry correction since ρ depends very little on z_A for a given \mathcal{Z} . For distances larger than $1 \mu\text{m}$, ρ may be well approximated by the CP formula [Eq. (29)]. This statement holds for the case of silicon but the results for gold surfaces (not shown) are even closer to the CP curve shown in Fig. 3.

Of course, finite conductivity corrections are very important for the evaluation of the force between an atom and a planar plate, and the full response function g has to be written as

$$g(k, z) = \rho(k, z) \eta_F F_{\text{CP}}^{(0)}. \quad (30)$$

In this formula, $F_{\text{CP}}^{(0)}$ is Casimir-Polder force (24), $\eta_F = F^{(0)}/F_{\text{CP}}^{(0)}$ represents the reduction in the dispersive force due to material properties of atom and surface (calculated for a plane geometry), and ρ describes the effect of geometry.

In Fig. 4, we plot η_F as a function of z_A for a Rb atom on top of a silicon or gold surface. As expected, the CP result for perfect reflectors is recovered at large distances in the case of gold, whereas for silicon we find a reduction in $\eta_F \sim 2/3$ due to the finite value of the zero-frequency permittivity in this case. These results coincide with those obtained in [46]. For both gold and silicon surfaces, the reduction gets stronger as the separation distance is decreased, as expected since shorter distances correspond to larger frequencies, for which the optical responses of both atom and surface are smaller. For very short distances, η_F is linear [$\eta_F \approx 5.8z$ (μm) for gold and $5.1z$ (μm) for silicon], in agreement with the power-law modification expected in the van der Waals unretarded regime.

Since ρ is well approximated by the Casimir-Polder result for perfect reflectors [Eq. (29)], the real material and beyond-PFA geometry corrections are approximately uncorrelated. One may compute the former effect for the simple plane geometry [$\eta_F(z_A)$], the latter for “perfect” atom and surface

[$\rho_{\text{CP}}^{\text{perf}}(kz_A)$], and finally combine the two effects with the help of Eq. (30). The simple analytical formula (29) is thus of great practical relevance since it allows for an easy evaluation of the response function $g(k, z_A)$. For a given corrugation wavelength, as was discussed in connection with Fig. 2, the two effects are more relevant at different separation ranges: η_F is mainly affected for small z_A (producing the linear increase in all curves on the left part of Fig. 2), whereas $\rho(k, z)$ differs for large kz_A (leading to the exponential decay apparent on the right part of Fig. 2). When k is small enough (as in the example with $\lambda = 10 \mu\text{m}$ on Fig. 2), the two regions do not overlap, explaining why the maximum can approach unity. Otherwise (as in the example with $\lambda = 100 \text{ nm}$ on Fig. 2), they do overlap and the maximum value of the curve remains well below unity.

Only for very short separation distances (or very short corrugation wavelengths for a given kz_A) $\rho(k, z_A)$ starts to deviate slightly from $\rho_{\text{CP}}^{\text{perf}}(kz_A)$, as illustrated by the light blue/gray curve in Fig. 3 for $z = 100 \text{ nm}$, resulting in some entanglement between real material and geometry corrections. In this case, ρ is well approximated by the van der Waals analytical formula derived in Appendix C.

V. EXPERIMENTAL PROSPECTS

There are several possible experimental scenarios where nontrivial geometrical effects of atom-surface forces could be probed. In particular, Bose-Einstein condensates represent an ideal sensor of quantum vacuum forces since they are well controlled and characterized. One possible experiment is to use a BEC as a sensitive oscillator, whose center-of-mass frequency is modified when the BEC is close to a surface [14]. This idea was recently used to measure the normal component of the Casimir-Polder force between a Rb condensate oscillating along the perpendicular direction to a planar dielectric surface [7]. Lateral Casimir-Polder forces could be measured in a similar fashion with an elongated BEC oscillating parallel to the surface, with its long axis parallel to the corrugation axis of a uniaxial corrugated surface [18,19]. We have shown in these references that nontrivial geometrical quantum vacuum effects, beyond the usual proximity force and pairwise summation approximations, could be measured using present-day cold-atom technology. We shall not further discuss this proposal here.

Rather, let us comment briefly on another possible scenario, which, although less sensitive, has the nice feature of measuring directly the atom-surface interaction potential instead of its second derivative, as in the BEC oscillator. The idea is to use a quasi-one-dimensional (1D) BEC to locally probe potential variations via imaging the local one-dimensional density. Small electric and magnetic fields of BECs in atom chips have been recently probed using this technique [54]. Lateral Casimir-Polder forces could be measured with a cigar-shaped BEC placed parallel to the surface and with its long axis perpendicular to the uniaxial corrugation lines. The potential along the quasi-one-dimensional BEC is related to the one-dimensional particle density $n_{1D}(x)$ as

$$V_{\text{ho}}(x) + V_{\text{CP}}(x) = -\hbar\omega_{\text{tr}}\sqrt{1 + 4a_{\text{scat}}n_{1\text{D}}(x)}, \quad (31)$$

where $V_{\text{ho}}(x)$ is the external harmonic trapping potential, $V_{\text{CP}}(x)$ is the lateral Casimir-Polder potential, ω_{tr} is the transverse (strong) trapping frequency, and a_{scat} is the s -wave scattering length. In [54] the optimal potential single-shot sensitivity ΔV is estimated as $\Delta V = \gamma\Delta N/\rho_0^2x_0$, where $\gamma = 2\hbar^2a_{\text{scat}}/m$. Here m is the mass of Rb atoms, ΔN is the detection imaging noise, x_0 is the longitudinal spatial resolution, and ρ_0 is the transverse spatial resolution. In the experiment [54], $\omega_{\text{tr}} = 2\pi \times 300$ Hz, $\Delta N \approx 4$ atoms per pixel in a charge-coupled device camera, leading to a single-shot single-point sensitivity to potential variations in $\Delta V \approx 10^{-13} - 10^{-14}$ eV.

For the sake of estimating the order of magnitude of the lateral Casimir-Polder force, let us consider a uniaxial corrugated perfectly reflecting surface. We now use our perturbative expansion of the potential in powers of the corrugation profile. In the retarded regime ($z_A \gg \lambda_A$), the zeroth-order potential is $U^{(0)}(z_A) = -3\hbar c\alpha(0)/32\pi^2\epsilon_0z_A^4$, where $\alpha(0)/4\pi\epsilon_0 = 47.3 \times 10^{-30}$ m³ for ⁸⁷Rb atoms. For a corrugation amplitude $h = 100$ nm, wavelength $\lambda = 10$ μm , and an atom-plate distance $z_A = 2$ μm , the correction is $U^{(1)} = 1.13 \times 10^{-14}$ eV, which is on the border of the experimental sensitivity reported in [54]. The experimental signal of the lateral Casimir-Polder force would consist of a density modulation of 1D BEC density following the law $n_{1\text{D}}(x) \approx [V_{\text{ho}}(x) + V_{\text{CP}}(x)]^2$.

Other possible experiments to probe lateral Casimir-Polder forces could involve spin-echo techniques for atomic beams flying above corrugated surfaces [4], a two-component phase-separated BEC "level" [55] used as a cold-atom analog of an atomic-force microscope (AFM) to map the corrugated surface potential, or two-photon Bragg spectroscopy of the Casimir-modified Bogoliubov spectrum of an elongated BEC above the surface [56].

VI. CONCLUSIONS

We have developed a scattering approach to the dispersive force between a ground-state atom and a material body. We have focused on the case of a corrugated surface, and derived explicit results to first order in the corrugation amplitude. Exact numerical calculation of the dispersive first-order potential has been presented in terms of the response function $g(k, z_A)$, calculated for arbitrary values of the separation distance z_A and corrugation wavelength $\lambda = 2\pi/k$, as long as the corrugation amplitude remains much smaller than both length scales. Different atomic species and materials can be considered within our formalism. Here we have illustrated our method by taking Rb atoms on top of gold or silicon surfaces.

For separation distances larger than 1 μm , the response function $g(k, z)$ can be easily obtained from the very simple CP result [Eq. (29)] for the beyond-PFA geometry correction factor ρ , together with the numerical values for the real material reduction factor η_F calculated for the plane geometry.

The position dependence of the resulting potential leads to a lateral dispersive force. We have discussed a variety of

possible experiments with Bose-Einstein condensates that would allow for the verification of nontrivial beyond-PFA effects with current state-of-the-art techniques.

ACKNOWLEDGMENTS

We are grateful to James Babb for providing us with the dynamic polarizability data for rubidium. R.M. acknowledges partial financial support by Ministero dell'Università e della Ricerca Scientifica e Tecnologica and by Comitato Regionale di Ricerche Nucleari e di Struttura della Materia. P.A.M.N. thanks CNPq, CAPES, and FAPERJ for financial support, and ENS for a visiting professor position. A.L. acknowledges financial support from the French Carnot Institute LETI. D.A.R.D acknowledges financial support from the U.S. Department of Energy through the LANL/LDRD Program. Part of this work was carried out at the Kavli Institute for Theoretical Physics, with support from NSF Grant No. PHY05-51164.

APPENDIX A: SCATTERING MATRIX FOR AN ATOMIC MAGNETIC-DIPOLE MOMENT

Equation (9) gives the expression of the atomic reflection matrix elements under the assumption that the atom is characterized by an electrical polarizability $\alpha(\omega)$. The expression of the matrix elements of the operator \mathcal{R}_A was found starting from the linear relation (5) between the induced atomic electric dipole and the external (incoming) electric field calculated in the position \mathbf{R}_A , and writing down the electric field produced by the induced dipole moment $\mathbf{d}(\omega)$. In particular, we were interested in the field going toward the surface (\downarrow) as a function of the field coming from it (\uparrow).

A completely analogous calculation can be performed assuming that the fluctuating magnetic field \mathbf{H} induces a magnetic-dipole moment \mathbf{m} on the atom given by

$$\mathbf{m}(\omega) = \beta(\omega)\mathbf{H}(\mathbf{R}_A, \omega), \quad (\text{A1})$$

where $\beta(\omega)$ is the magnetic polarizability. For the field generated by the magnetic dipole in the region $z < z_A$ we find the Fourier component

$$E_{(\text{mdip})p}^\downarrow(\mathbf{k}, \omega) = -\frac{i\omega}{2\epsilon_0c^2k_z}e^{-i\mathbf{k}\cdot\mathbf{r}_A}e^{ik_zz_A} \times \hat{\boldsymbol{\epsilon}}_p^-(\mathbf{k}) \cdot [\mathbf{K}^- \times \mathbf{m}(\omega)]. \quad (\text{A2})$$

Using the following expression for the magnetic field coming upward from the surface

$$\mathbf{H}^\uparrow(\mathbf{k}, z, \omega) = \frac{1}{\mu_0\omega} \sum_p E_p^\uparrow(\mathbf{k}, \omega) [\mathbf{K}^+ \times \hat{\boldsymbol{\epsilon}}_p^+(\mathbf{k}, \omega)] e^{ik_zz}, \quad (\text{A3})$$

and replacing Eq. (A1) into expression (A2) we find

$$\begin{aligned} \langle \mathbf{k}, p | \mathcal{R}_A^m | \mathbf{k}', p' \rangle = & -\frac{\beta(i\xi)}{2\kappa} e^{-i(\mathbf{k}-\mathbf{k}')\cdot\mathbf{r}_A} e^{-(\kappa+\kappa')z_A} \\ & \times \hat{\boldsymbol{\epsilon}}_p^-(\mathbf{k}, i\xi) \cdot \{\mathbf{K}^- \times [\mathbf{K}'^+ \times \hat{\boldsymbol{\epsilon}}_{p'}^+(\mathbf{k}', i\xi)]\}. \end{aligned} \quad (\text{A4})$$

As a consequence, if we want to include both contributions

(electric- and magnetic-dipole moments), the atomic reflection operator is simply given by the sum of the operators \mathcal{R}_A and \mathcal{R}_A^M , given by Eqs. (9) and (A4), respectively. It is possible to check, for example, that for two atoms the scattering formula (4) gives back the known result for the interatomic potential energy in the Casimir-Polder regime [45].

APPENDIX B: CASIMIR-POLDER REGIME

Simple closed forms for the first-order response function can be derived in some limiting cases. In fact, $g(k, z_A)$ is given by the integral over the positive imaginary frequency axis of a function involving three quantities that decay to zero: the atomic polarizability $\alpha(i\xi)$, the round-trip propagation factor $\exp[-(\kappa' + \kappa'')z_A]$, and the reflection amplitudes $r^p(k, i\xi)$ (due to the frequency dependence of the permittivity function). These functions decay on different frequency scales: c/λ_A , c/z_A , and ω_p (a typical frequency associated to the surface optical response, for example, the plasma frequency for metallic media), respectively. As a consequence, the significant range of frequencies giving the main contribution to the integral in Eq. (17) will be determined by the smallest of these frequency scales. One can then expect that the integral (17) can be considerably simplified for some particular relations between these frequency scales.

In this appendix, we consider the case $z_A \gg \lambda_p, \lambda_A$, usually referred to as Casimir-Polder regime [note that we assume $z_A \ll \hbar c/(k_B T)$ so as to neglect thermal corrections]. Since the smallest frequency scale is c/z_A , we can replace the dynamical polarizability $\alpha(i\xi)$ and the permittivity $\epsilon(i\xi)$ by their zero-frequency values. For the metallic case, we can take $\epsilon(0) \rightarrow \infty$ and then derive remarkably simple expressions from Eq. (23):

$$a_{\mathbf{k}', \mathbf{k}''} = \frac{1}{2} e^{-(\kappa' + \kappa'')z_A} \left\{ \frac{1}{\kappa' \kappa''} [k^2 + (\kappa' - \kappa'')^2] + \frac{c^2}{\xi^2} [k^2 - (\kappa' + \kappa'')^2] \right\}. \quad (\text{B1})$$

This expression could also have been obtained by taking the usual perfectly reflecting boundary conditions on the corrugated surface.

After replacing Eq. (B1) into

$$g_{\text{CP}}(k, z_A) = \frac{\hbar \alpha(0)}{\epsilon_0 c^2} \int_0^\infty \frac{d\xi}{2\pi} \xi^2 \int \frac{d^2 \mathbf{k}'}{(2\pi)^2} a_{\mathbf{k}', \mathbf{k}''}(z_A, \xi),$$

we change the integration variables from (ξ, k', ϕ') to $(\kappa', \kappa'', \phi)$, taking $k'(\kappa', \kappa'', \phi) = [(\kappa')^2 - (\kappa'')^2 + k^2]/(2k \cos \phi')$ and $\xi(\kappa', \kappa'', \phi) = c[(\kappa')^2 - (\kappa'')^2 - (\kappa' \kappa'')^2]^{1/2}$. The Jacobian of the transformation is $|J| = 2c\kappa' \kappa'' / \{4k^2(\kappa')^2 \cos^2 \phi' - [(\kappa')^2 - (\kappa'')^2 + k^2]^2\}^{1/2}$. We first use the property $\int_0^{2\pi} d\phi'(\dots) = 2 \int_0^\pi d\phi'(\dots)$. Then we write the integral as a sum of two contributions:

$$\int_0^\infty d\kappa' \int_{|\kappa' - k|}^{\sqrt{(\kappa')^2 + k^2}} d\kappa'' \int_0^{\phi_m} d\phi',$$

and

$$\int_0^\infty d\kappa' \int_{\sqrt{(\kappa')^2 + k^2}}^{\kappa' + k} d\kappa'' \int_{\phi_m}^\pi d\phi',$$

with $\cos \phi_m = [(\kappa')^2 - (\kappa'')^2 + k^2]/2\kappa' k$, and introduce further auxiliary integration variables $u = \kappa' + \kappa''$ and $v = \kappa' - \kappa''$ to obtain the final analytical result

$$g_{\text{CP}}^{\text{perf}}(k, z_A) = F_{\text{CP}}^{(0)}(z_A) e^{-\mathcal{Z}} \left(1 + \mathcal{Z} + \frac{16\mathcal{Z}^2}{45} + \frac{\mathcal{Z}^3}{45} \right), \quad (\text{B2})$$

where $\mathcal{Z} \equiv kz_A$.

APPENDIX C: VAN DER WAALS REGIME

In this appendix, we assume that $z_A \ll \lambda_A$. In this van der Waals regime, one can neglect retardation effects and assume an instantaneous atom-surface interaction (limit $c \rightarrow \infty$).

In order to extract some simple expressions for the vdW response function, we have first to choose a specific expression for the atomic polarizability $\alpha(i\xi)$. We will use the following model function suitable for a multilevel isotropic atom having transition frequencies ω_{n0} from the n th excited state to the ground-state and electric-dipole matrix elements d_{n0} on these transitions

$$\alpha(i\xi) = \frac{2}{3\hbar} \sum_n \frac{\omega_{n0} d_{n0}^2}{\omega_{n0}^2 + \xi^2}, \quad (\text{C1})$$

Then we have to specify the transmission and reflection amplitude functions. Here we take Fresnel formulas with two different models for the permittivity $\epsilon(i\xi)$.

1. Plasma metals

We first take the plasma model for metallic materials,

$$\epsilon(i\xi) = 1 + \frac{\omega_p^2}{\xi^2}. \quad (\text{C2})$$

In this case we obtain from Eqs. (17)–(23)

$$g_{\text{vdW}}(k, z_A) = - \sum_n \frac{k d_{n0}^2 x_n}{192 \sqrt{2} \pi \epsilon_0 z_A^3 (x_n^2 + 2\sqrt{2}x_n + 2)} \{ 6\sqrt{2} \mathcal{Z}(x_n) + \sqrt{2} K_0(\mathcal{Z}) + [\sqrt{2}(\mathcal{Z}^2 + 12)x_n + \mathcal{Z}^2 + 24] K_1(\mathcal{Z}) \}, \quad (\text{C3})$$

where $x_n = \omega_p / \omega_{n0}$ and $\mathcal{Z} = kz_A$, and K_0 and K_1 are the modified Bessel functions [53]. If we let all the x_n go to infinity, we get the result for a perfect conductor [19]

$$g_{\text{vdW}}^{\text{perf}}(k, z_A) = - \sum_n \frac{k d_{n0}^2}{192 \pi \epsilon_0 z_A^3} [6\mathcal{Z} K_0(\mathcal{Z}) + (\mathcal{Z}^2 + 12) K_1(\mathcal{Z})]. \quad (\text{C4})$$

In the opposite limit, with $\omega_p \ll \omega_{n0}$ for all n , we derive from Eq. (C3) the plasmon van der Waals limit

$$g_{\text{vdW}}^{\text{plas}}(k, z_A) = - \sum_n \frac{k d_{n0}^2 x_n}{384 \sqrt{2} \pi \epsilon_0 z_A^3} [12 \mathcal{Z} K_0(\mathcal{Z}) + (\mathcal{Z}^2 + 24) K_1(\mathcal{Z})]. \quad (\text{C5})$$

This result is, as expected, proportional to the plasma frequency ω_p .

2. Semiconductors

In order to treat the case of semiconductors, we assume that the material can be described by the Drude-Lorentz model function

$$\epsilon(i\xi) = 1 + \frac{\omega_{DL}^2 [\epsilon(0) - 1]}{\omega_{DL}^2 + \xi^2}. \quad (\text{C6})$$

In this case we get

$$g_{\text{vdW}}(k, z_A) = - \sum_n \frac{\gamma k d_{n0}^2 x_n}{384 \epsilon \pi \epsilon_0 z_A^3 (\gamma + 2)^{3/2} [(\gamma + 2) x_n^2 - 2]^2} \times [12 A_0 \mathcal{Z} K_0(\mathcal{Z}) + A_1(\mathcal{Z}) K_1(\mathcal{Z})],$$

$$A_0 = (\gamma + 2)(\sqrt{\gamma + 2} x_n - \sqrt{2})[(\gamma + 2) x_n^2 - 2],$$

$$A_1 = 2(\gamma + 2)^{3/2} [(\mathcal{Z}^2 + 12)\gamma + 24] x_n^3 - 3\sqrt{2}(\gamma + 2)[(\mathcal{Z}^2 + 8)\gamma + 16] x_n^2 - 48(\gamma + 2)^{3/2} x_n + 2\sqrt{2}[(\mathcal{Z}^2 + 24)\gamma + 48], \quad (\text{C7})$$

where $\gamma = \epsilon(0) - 1$ and $x_n = \omega_{DL} / \omega_{n0}$.

-
- [1] C. I. Sukenik, M. G. Boshier, D. Cho, V. Sandoghdar, and E. A. Hinds, *Phys. Rev. Lett.* **70**, 560 (1993).
- [2] A. Landragin, J. Y. Courtois, G. Labeyrie, N. Vansteenkiste, C. I. Westbrook, and A. Aspect, *Phys. Rev. Lett.* **77**, 1464 (1996).
- [3] F. Shimizu, *Phys. Rev. Lett.* **86**, 987 (2001).
- [4] V. Druzhinina and M. DeKieviet, *Phys. Rev. Lett.* **91**, 193202 (2003).
- [5] T. A. Pasquini, Y. Shin, C. Sanner, M. Saba, A. Schirotzek, D. E. Pritchard, and W. Ketterle, *Phys. Rev. Lett.* **93**, 223201 (2004); T. A. Pasquini, M. Saba, G. Jo, Y. Shin, W. Ketterle, D. E. Pritchard, T. A. Savas, and N. Mulders, *ibid.* **97**, 093201 (2006).
- [6] D. M. Harber, J. M. Obrecht, J. M. McGuirk, and E. A. Cornell, *Phys. Rev. A* **72**, 033610 (2005).
- [7] J. M. Obrecht, R. J. Wild, M. Antezza, L. P. Pitaevskii, S. Stringari, and E. A. Cornell, *Phys. Rev. Lett.* **98**, 063201 (2007).
- [8] Y. J. Lin, I. Teper, C. Chin, and V. Vuletic, *Phys. Rev. Lett.* **92**, 050404 (2004).
- [9] *Conference on Atoms and Molecules Near Surfaces (CAMS)J. Phys.:* Conf. Ser. 19 (2005).
- [10] H. B. G. Casimir and D. Polder, *Phys. Rev.* **73**, 360 (1948).
- [11] F. S. S. Rosa, D. A. R. Dalvit, and P. W. Milonni, *Phys. Rev. A* **78**, 032117 (2008).
- [12] L. P. Pitaevskii, *Phys. Rev. Lett.* **101**, 163202 (2008).
- [13] S. Y. Buhmann and D.-G. Welsch, *Prog. Quantum Electron.* **31**, 51 (2007), and references therein.
- [14] M. Antezza, L. P. Pitaevskii, and S. Stringari, *Phys. Rev. Lett.* **95**, 113202 (2005).
- [15] V. Druzhinina, M. Mudrich, F. Arnecke, J. Madroñero, and A. Buchleitner, e-print arXiv:0810.4281.
- [16] B. V. Derjaguin and I. I. Abrikosova, *Sov. Phys. JETP* **3**, 819 (1957); B. V. Derjaguin, *Sci. Am.* **203**, 47 (1960).
- [17] See, for instance, V. B. Bezerra, G. L. Klimchitskaya, and C. Romero, *Phys. Rev. A* **61**, 022115 (2000).
- [18] D. A. R. Dalvit, P. A. Maia Neto, A. Lambrecht, and S. Reynaud, *J. Phys. A: Math. Theor.* **41**, 164028 (2008).
- [19] D. A. R. Dalvit, P. A. Maia Neto, A. Lambrecht, and S. Reynaud, *Phys. Rev. Lett.* **100**, 040405 (2008).
- [20] H. B. Chan, Y. Bao, J. Zou, R. A. Cirelli, F. Klemens, W. M. Mansfield, and C. S. Pai, *Phys. Rev. Lett.* **101**, 030401 (2008). The exact solution for the Casimir force in this configuration has been recently found using the scattering approach in.
- [21] A. Lambrecht and V. N. Marachevsky, *Phys. Rev. Lett.* **101**, 160403 (2008).
- [22] J. F. Babb, G. L. Klimchitskaya, and V. M. Mostepanenko, *Phys. Rev.* **70**, 042901 (2004).
- [23] M. Babiker and G. Barton, *J. Phys. A* **9**, 129 (1976).
- [24] J. M. Wylie and J. E. Sipe, *Phys. Rev. A* **30**, 1185 (1984).
- [25] S. Y. Buhmann, D.-G. Welsch, and T. Kampf, *Phys. Rev. A* **72**, 032112 (2005).
- [26] B. Döbrich, M. DeKieviet, and H. Gies, *Phys. Rev. D* **78**, 125022 (2008).
- [27] E. M. Lifshitz, *Sov. Phys. JETP* **2**, 73 (1956).
- [28] I. E. Dzyaloshinskii and L. P. Pitaevskii, *Sov. Phys. JETP* **9**, 1282 (1959); I. E. Dzyaloshinskii, E. M. Lifshitz, and L. P. Pitaevskii, *Adv. Phys.* **10**, 165 (1961).
- [29] E. I. Kats, *Sov. Phys. JETP* **46**, 109 (1977).
- [30] A. Lambrecht, P. A. Maia Neto, and S. Reynaud, *New J. Phys.* **8**, 243 (2006).
- [31] M. T. Jaekel and S. Reynaud, *J. Phys. I* **1**, 1395 (1991)
- [32] C. Genet, A. Lambrecht, and S. Reynaud, *Phys. Rev. A* **67**, 043811 (2003).
- [33] P.A. Maia Neto, A. Lambrecht, and S. Reynaud, *Europhys. Lett.* **69**, 924 (2005); *Phys. Rev. A* **72**, 012115 (2005). The second paper contains a typo in Eq. (36) since the matrix $\Lambda^{(1)}$ is expressed as $\Lambda_-^{(1)} - \Lambda_+^{(1)}$. The correct formula, with + and - exchanged, is the expression given in the present paper.
- [34] R. B. Rodrigues, P. A. Maia Neto, A. Lambrecht, and S. Reynaud, *Phys. Rev. Lett.* **96**, 100402 (2006); *Phys. Rev. A* **75**, 062108 (2007).
- [35] A. Bulgac, P. Magierski, and A. Wirzba, *Phys. Rev. D* **73**, 025007 (2006).
- [36] M. Bordag, *Phys. Rev. D* **73**, 125018 (2006).
- [37] T. Emig, *J. Stat. Mech.: Theory Exp.* **2008**, P04007.
- [38] P. A. Maia Neto, A. Lambrecht, and S. Reynaud, *Phys. Rev. A* **78**, 012115 (2008).
- [39] T. Emig, N. Graham, R. L. Jaffe, and M. Kardar, *Phys. Rev.*

- Lett. **99**, 170403 (2007).
- [40] O. Kenneth and I. Klich, Phys. Rev. B **78**, 014103 (2008).
- [41] Dimensionally speaking, $\alpha(\omega)$ is equal to $4\pi\epsilon_0$ times a volume. The latter volume [i.e., $\alpha(\omega)/4\pi\epsilon_0$] is identified with the polarizability in “electrostatic cgs” convention, used in a number of papers studying dispersion forces. This point has to be treated carefully when comparing various expressions.
- [42] M. Nieto-Vesperinas, *Scattering and Diffraction in Physical Optics* (Wiley, New York, 1991).
- [43] R. Carminati, M. Nieto-Vesperinas, and J.-J. Greffet, J. Opt. Soc. Am. A Opt. Image Sci. Vis. **15**, 706 (1998).
- [44] For consistency, higher-order multipoles beyond the electric-dipole approximation for the atom-field coupling would also be needed to compute corrections involving higher powers of \mathcal{R}_A .
- [45] G. Feinberg and J. Sucher, Phys. Rev. A **2**, 2395 (1970).
- [46] M. Antezza, L. P. Pitaevskii, and S. Stringari, Phys. Rev. A **70**, 053619 (2004).
- [47] J.-J. Greffet, Phys. Rev. B **37**, 6436 (1988).
- [48] G. S. Agarwal, Phys. Rev. B **15**, 2371 (1977).
- [49] The procedure to compute $\alpha(i\omega)$ is described in A. Derevianko, W. R. Johnson, M. S. Safronova, and J. F. Babb, Phys. Rev. Lett. **82**, 3589 (1999) (see also references therein). The authors used *ab initio* relativistic methods, taking experimental values for the atomic energy differences, and both theoretical and experimental values for the electric-dipole matrix elements. The resulting numerical data were kindly provided by Babb to many research groups. They can be found, for example, in Fig. 9 of [46].
- [50] *Handbook of Optical Constants of Solids*, in edited by E. Palik (Academic Press, New York, 1998).
- [51] A. Lambrecht and S. Reynaud, Eur. Phys. J. D **8**, 309 (2000).
- [52] I. Pirozhenko and A. Lambrecht, Phys. Rev. A **77**, 013811 (2008).
- [53] *Handbook of Mathematical Functions*, edited by M. Abramowitz and I. Stegun (Dover, New York, 1972).
- [54] S. Wildermuth, S. Hofferberth, I. Lesanovsky, E. Haller, L. M. Anderson, S. Groth, I. Bar-Joseph, P. Krüger, and J. Schmiedmayer, Nature (London) **435**, 440 (2005); P. Krüger, S. Wildermuth, S. Hofferberth, L. M. Anderson, S. Groth, I. Bar-Joseph, and J. Schmiedmayer, J. Phys.: Conf. Ser. **19**, 56 (2005); S. Wildermuth, S. Hofferberth, I. Lesanovsky, S. Groth, P. Krüger, J. Schmiedmayer, and I. Bar-Joseph, Appl. Phys. Lett. **88**, 264103 (2006).
- [55] S. G. Bhongale and E. Timmermans, Phys. Rev. Lett. **100**, 185301 (2008).
- [56] G. Moreno, D. A. R. Dalvit, and E. Calzetta, e-print arXiv:0904.0238.